Chemical Research in Toxicology

DECEMBER 2000
VOLUME 13, NUMBER 12

Articles

An Adjacent Thioester Provides Apical-Directed Stabilization to 3-Isothiazolidinone 1-Oxide Heterocycles

Roman Reznik and Alexander Greer*

Department of Chemistry, Graduate School, and University Center, The City University of New York, Brooklyn College, Brooklyn, New York 11210

Received June 13, 2000

The structural and energetic features of the attractive intramolecular through-space S−X interaction [X being oxygen (O) or sulfur (S)] of thioester containing 3-isothiazolidinone 1-oxide heterocycles are described. Density functional theoretical and semiempirical calculations are used to explain the previous X-ray data on 3-isothiazolidinone 1-oxides **5** and **6** [Kanda, Y., Ashizawa, T., Kakita, S., Takahashi, Y., Kono, M., Yoshida, M., Saitoh, Y., and Okabe, M. (1999) *J. Med. Chem.* **42**, 1330−1332] and implicate a mechanism where the adjacent thioester participates in an apical-directed stabilization of the sulfur heterocycle. A key factor that distinguishes the S−O interaction from the S−S interaction is the stronger through-space interaction of the former, which is a consequence of the greater electronegativity of apical O compared to apical S. Reaction field theory reveals that the conversion of the S−O interaction to the S−S interaction is more facile compared to gas phase computations, which suggest a reduced importance of the 1,5-S−X interactions in solution. The conversion of the S−O interaction to the S−S interaction gives an isothiazolidinone oxide that places the reacting sulfurs in proximity with an orientation presumably suitable for bond formation and access to the dithiolanone oxide surface. Factors that influence the through-space S−X interactions may represent important issues in identifying target 3-isothiazolidinone 1-oxide prodrugs capable of rearranging to 1,2-dithiolan-3-one 1-oxide drugs.

Introduction

The 1,2-dithiolan-3-one 1-oxide heterocycle is found in the natural product leinamycin **1** and the synthetic analogues **2**−**4** (Scheme 1) (*1*, *2*). Recent studies suggest that 1,2-dithiolan-3-one 1-oxide is also produced in situ from the unimolecular rearrangement of thioester-containing 3-isothiazolidinone 1-oxides, such as **5** and **6** (*3*). While the general mechanism for the conversion of 3-isothiazolidinone 1-oxide to 1,2-dithiolan-3-one 1-oxide is yet to be established, interest has surrounded dithiolanone oxide **1** (leinamycin) because of its potent antitumor activity and unusual DNA-cleaving behavior (*1*, *4*−*7*). Elegant studies by Gates and co-workers led to the mechanistic proposal that leinamycin reacts with thiol to produce polysulfides (RSS_xSR), which in the presence

* To whom correspondence should be addressed. E-mail: agreer@brooklyn.cuny.edu.

10.1021/tx000126+ CCC: $19.00
Published on Web 11/18/2000

Scheme 1

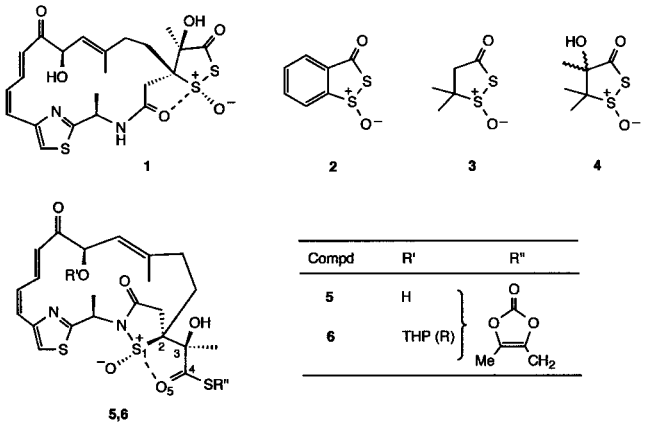

Scheme 2

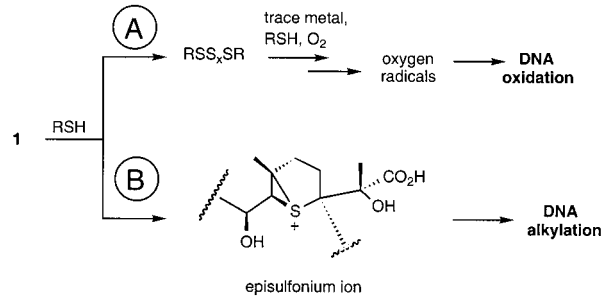

of DNA and molecular oxygen give rise to DNA damage by oxygen radicals from a trace metal-dependent Fenton reaction (Scheme 2A) (*7*). It was noted that a dual mechanism to DNA damage may exist (Scheme 2A,B) (*7*) since the reaction of leinamycin with thiol also generates an intermediate, presumably episulfonium ion, which can form a covalent bond with DNA (*8*, *9*).

In an effort to generate 1,2-dithiolan-3-one 1-oxides in vivo, Kanda and co-workers investigated a variety of thioester derivatives of leinamycin (e.g., **5** and **6**) (*3*). It was reported that 3-isothiazolidinone 1-oxide **6** forms the six-membered ring sulfide **8** as well as initiates antiproliferative and antitumor activity (Scheme 3) (*3*). Although not isolated, the intermediate thought to be responsible for the biological activity is dithiolanone oxide (**7**). The fact that isothiazolidinone oxide **6** is more stable to decomposition than dithiolanone oxide **1** in phosphate buffer/acetonitrile (4:1) [$t_{1/2}$ = 30 h (**6**) and 6 h (**1**)] may signal a clinical potential for **6**. This unveils the need for more detailed studies of isothiazolidinone oxides as potential precursors to dithiolanone oxides.

We report here a computational study that attempts to discover factors that determine isothiazolidinone oxide stability. With an understanding of the structural elements of isothiazolidinone oxides, predictions about the controlled conversion to dithiolanone oxide become possible. On the basis of density functional theoretical and semiempirical calculations and analyses of previous experimental X-ray data, we find that stability depends on the hitherto unreported attractive through-space 1,5-sulfur−X (S−X) interaction (X being oxygen or sulfur) between the adjacent thioester and the isothiazolidinone oxide heterocycle (Scheme 4). The bond between C4 and X5 in Scheme 4 can be either a single bond or a double bond. This study examines gas phase and solution phase reactions. The gas phase reactions favor dipole−dipole

Scheme 3

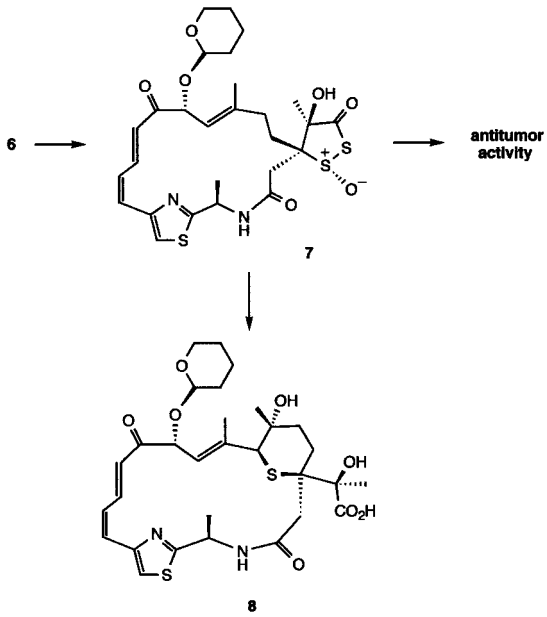

Scheme 4

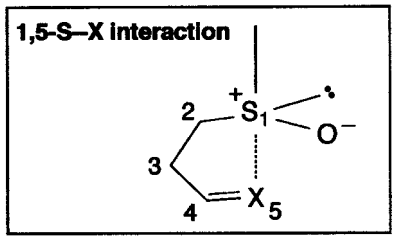

stabilization and intramolecular hydrogen bonding. Solvent effects are found to reduce the importance of the 1,5-S−X interactions because of the potential for specific hydrogen bonding interaction with the solute. This study explains the 1,5-S−O interaction relevant in the crystal data of isothiazolidinone oxide **5** and **6** (*3*) and implicates a mechanism where the adjacent thioester participates in an apical-directed stabilization of the sulfur heterocycle. Factors that influence the through-space S−X interactions may become important issues in identifying target isothiazolidinone oxides that are susceptible to collapse to dithiolanone oxide.

Results and Discussion

Many X-ray crystal structures possess 1,5-intramolecular S−X interactions (X being oxygen or sulfur) (*10*), of which the structures of isothiazolidinone oxide **5** and **6** are included (*3*). There is a dearth of information pertaining to through-space S−X interactions in biochemistry (*11*−*14*); however, the influence of the 1,5-S−O interaction in leinamycin **1** has recently been described (*15*). We report here calculations at the B3LYP/6-31G* level (*16*) for **9** since this level is found to reproduce experimental X-ray structures of molecules with hypervalent sulfur centers. Polarized continuum model (PCM) and self-consistent reaction field (SCRF) single-point calculations (*17*, *18*) at the B3LYP/6-31G* level were performed on stationary points to model solvent effects. The solvent calculations were performed with 100 points per interlocking sphere. The dielectric constant of 80.10 was used to simulate an aqueous environment. Con-

Scheme 5

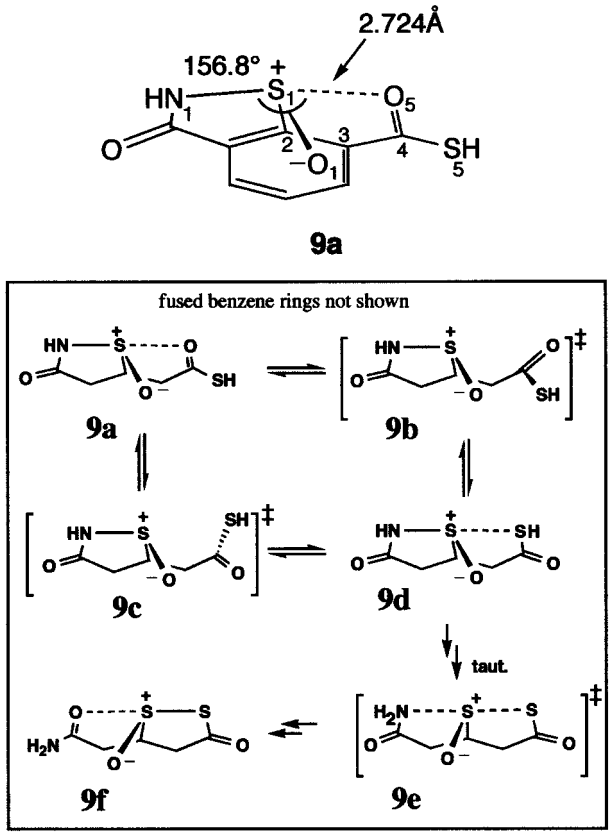

9a **9b** **9c** **9d** **9e** **9f**

strained B3LYP/6-31G*//B3LYP/3-21G calculations were conducted on **10**; these data were then transposed into the mixed anhydride core of **5** and **6**, followed by constrained optimizations with the semiempirical PM3 method. We report here a detailed theoretical study that describes the through-space 1,5-S−X interactions of thioester-containing isothiazolidinone oxides. The computational results and previous X-ray data taken together provide evidence for the enhanced stability of isothiazolidinone oxides engaged in through-space S−X contacts. The favorable S−X interaction corresponds to the preference for a trigonal bipyramidal (TBP) geometry at sulfur.

Model system **9a**−**f** provides for a simple example of the 1,5-S−X interactions (Scheme 5). Since 1,2-benzodithiol-3-one 1-oxide has been applied successfully as a DNA-cleaving model of leinamycin (*2*, *7*), we thought that a benzene-fused model, such as **9**, that possessed the potential for intramolecular 1,5-S−X interactions may mimic the key features of **5** and **6**. Geometry optimizations, vibrational frequencies, and internal reaction coordinates (IRCs) were performed for benzoisothiazolinone oxides **9a** and **9d** and transition structures **9b** and **9c**. Transition structure **9e** and dithiolanone oxide **9f** are included for reference, but their connectivity to **9a**−**d** is not elucidated. Structures **9a**−**f** possess either four or five bonds at the central sulfur (S1). Two different conformers (**9a** and **9d**) were identified by a search of conformational space (Figure 1). Conformer **9a** optimizes to a minimum where the S1 and O5 atoms are in close contact (2.800 Å). This calculated value is similar to the S−O nonbonded contact observed in the crystal structure of methyl [4-*tert*-butyl-2-methyl-1,2,3-thiadiazol-5(2*H*)-ylidene]acetate (2.518 Å, **11**) (Scheme 6) (*19*). The S1−O5 bond distance falls inside the van der Waals contact

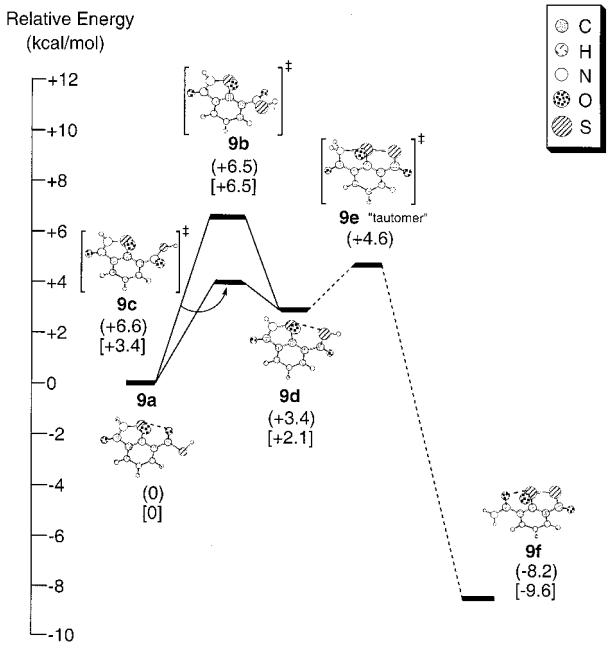

Figure 1. Compound **9** potential energy surface. The gas phase B3LYP/6-31G* energies are in parentheses, and the solution phase self-consistent reaction field calculations (SCRF), with single-point B3LYP/6-31G* calculations with dielectric constant of water ϵ of 80.10, are in brackets. Bond lengths (angstroms) and angles (degrees) are discussed in the text.

Scheme 6

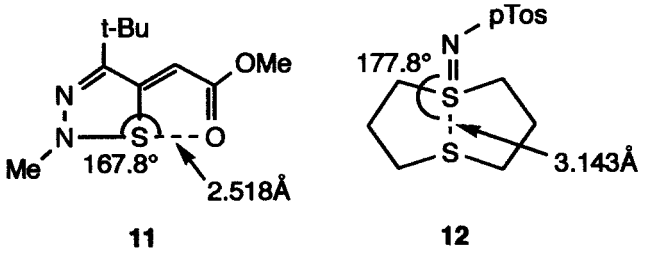

11 **12**

distance of the sulfur−oxygen bond (3.3 Å) (*18*) and outside of the covalent contact distance (1.8 Å) (*21*).

Conformer **9d** optimizes to a minimum where the S1 and S5 atoms are in close contact (3.263 Å). This is similar to the S−S contact observed in the crystal structure of 1-(tosylimino)-1,5-dithiacyclooctane (3.143 Å, **12**) (*22*). The calculated S−S bond distance of **9d** falls inside the van der Waals contact distance for the sulfur−sulfur bond (3.5 Å) (*20*) and outside of the covalent contact distance (*10*). The geometries of **9a** and **9d** are TBP at sulfur (S1) with the lone pair electrons equatorial and the oxygen (O5) or the sulfur (S5) apical. The N1−S1−O5 bond angle of **9a** (155.2°) and the N1−S1−S5 bond angle of **9d** (148.0°) are distorted compared to that of an ideal TBP geometry (180°) (*23*). B3LYP/6-31G* energies show that the reaction of **9a** and **9d** is endothermic by 3.4 kcal/mol. PCM solvation calculations predict that the endothermicity is reduced to 2.1 kcal/mol (details of the solvent calculations are given below). Coordination of the O5 or S5 ligands to S1 may play a key role in the stability and preferred geometry of the sulfur heterocycle since the structure is sensitive to the identity of the apical ligand X. The energetic difference between **9a** and **9d** can be understood in terms of the established preference for the apical position of oxygen compared to sulfur (*24*−*26*).

Benzoisothiazolinone oxide **9a** can convert to **9d** via transition structures **9b** and **9c,** calculated to be 6.5 and 6.6 kcal/mol, respectively, with gas phase B3LYP/6-31G* calculations. Transition structure (TS) **9b** is accessed by rotation of the thio acid group in a clockwise movement about the C4−O5 bond relative to the S1−C2 bond, while **9c** is accessed upon rotation in the opposite direction. The S−O and S−S bond distances of TSs **9b** and **9c** (3.728−4.165 Å) fall outside of the van der Waals contact distance. Consequently, TSs **9b** and **9c** are four-coordinate rather than six-coordinate, adopting tetrahedral geometries at S1 similar to that of a stable sulfoxides (*10*). The N1−S1−O1 bond angles of **9b** and **9c** are tetrahedral (111.0°) and pyramidal in nature. Predictions for the effect of solvent on the barrier to thio acid rotation were evaluated with single-point B3LYP calculations utilizing the self-consistent reaction field with B3LYP/6-31G*-optimized structures. When the dielectric constant of water is used in the continuum solvation model calculations, a reduced energy is observed for **9c** (3.4 kcal/mol), but not for **9b** (6.5 kcal/mol). A qualitative difference is observed in transition structures **9c** and **9b**; the reduced energy of **9c** cannot simply be attributed to solvation since structures **9a** and **9c** have similar dipole moments in the gas phase (3.96 D for **9a** and 3.85 D for **9c**) and the solution phase (7.07 D for **9a** and 6.73 D for **9c**). This is in contrast to the high-energy transition structure **9b**, which possesses a reduced dipole moment (2.45 D) in the gas phase compared to that in solution (4.09 D). We speculate that the relevant solution phase transition state will increase in energy because of solvent hydrogen bonding interactions, thus reducing the attractive effects of the 1,5-S−X interactions. Since the potential for specific hydrogen bonding interaction with the solute is not modeled here, one may argue that the effect of water as solvent is not well-reproduced. Estimating solvent effects for cases where the solvent gives a specific interaction with the solute, such as hydrogen bonding, is a challenging task (*27*, *28*).

Upon formation of isothiazolidinone oxide **9d**, the reacting sulfurs are in proximity with an orientation presumably suitable for S−S bond formation and access to the dithiolanone oxide surface. If it is assumed that nucleophilic addition and proton transfer occur prior to transition structure **9e**, the displacement of the amide to yield dithiolanone oxide **9f** could follow.[1] The computations lead us to suggest that intermediate **9d** is the reactive rotamer precursor to dithiolanone oxide. While connectivity between **9a**−**d** and **9e,f** is yet to be elucidated, indicated with dashed lines in Figure 1, it is significant that dithiolanone oxide **9f** is more stable than benzoisothiazolinone oxide **9a** by 8.2 kcal/mol in the gas phase and 9.6 kcal/mol according to PCM solvation calculations and represents the global minimum on the potential energy surface.

Model system **10a**−**d** was designed to mimic the S−X core of isothiazolidinone oxide **5** and **6**. Constrained geometry optimizations were conducted at the B3LYP/3-21G level with single-point calculations performed at the B3LYP/6-31G* level (Scheme 7 and Figure 2).[2] Six different conformers (**10a**−**d**, **10b′**, and **10c′**) were analyzed. These conformers display a similar activating effect to the benzofused system **9a**−**d**. Each conformer is related by approximate 60° rotation about the torsion angle θ (C2−C3−C4−O5). The constrained optimization of conformer **10a** reveals that the S1 and O5 atoms are in close contact (2.920 Å).[2] This calculated value is similar to the length of the S−O nonbonded contact observed in benzoisothiazolinone oxide **9a** (2.800 Å). Under the constraints imposed,[2] conformer **10d** optimizes to a minimum where the S1 and S5 atoms are in close contact (3.170 Å), which is similar to that of benzoisothiazolinone

Scheme 7

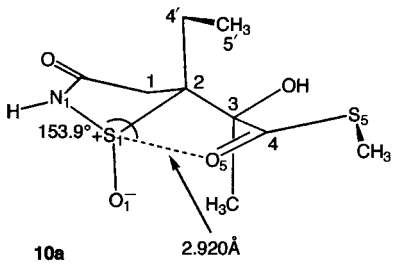

10a

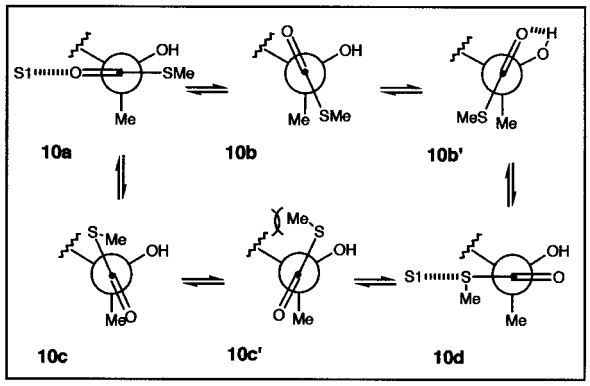

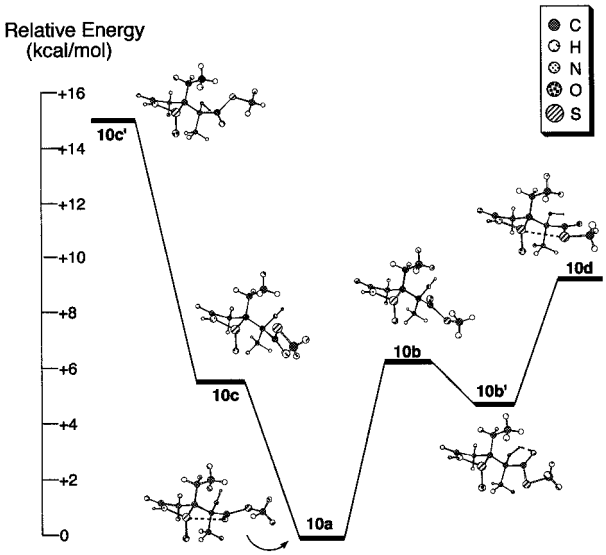

Figure 2. B3LYP/6-31G*//B3LYP/3-21G-optimized potential energy surface. Bond lengths (angstroms) and angles (degrees) are discussed in the text.

[1] We thank the reviewer for a comment on this part of the potential energy surface.

[2] The dihedral angles ϕ (C1−C2−C4′−C5′) and λ (C3−C2−C4′−C5′) were fixed at 175° and −65°, respectively. This computational procedure attempts to mimic the sterics factors involved in the 18-membered ring macrocycles **5** and **6**. The dihedral angle ϕ is positive for a clockwise movement from C1 to C5′ as you look down C2 to C4′. The dihedral angle λ is negative for a clockwise movement from C3 to C5′ as you look down C2 to C4′. The torsion angle θ (C2−C3−C4−O5) was constrained at approximate 60° intervals to reveal whether the S−X interaction intercedes in all or only some of the rotameric partners.

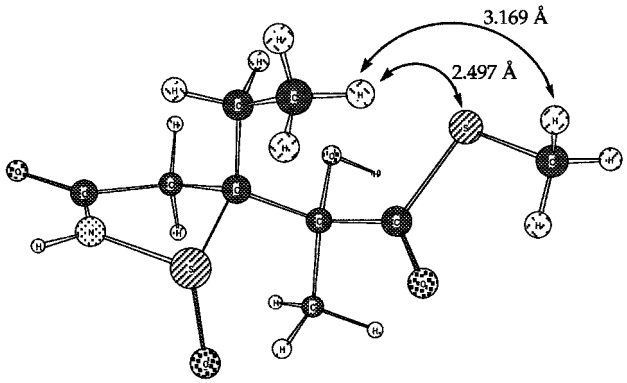

Figure 3. Rotamer **10c′** with the steric repulsion between the $-SCH_3$ group and ethyl group illustrated.

oxide **9d** (3.263 Å). Conformers **10a** and **10d** adopt TBP geometries at sulfur (S1) with the ligands O5 and S5 residing in the apical position. Gas phase B3LYP/6-31G-(d)//B3LYP/3-21G calculations show that the reaction of **10a** and **10d** is endothermic by 9.3 kcal/mol, which correlates to the established enhanced apocophilicity of oxygen compared to sulfur (*24*−*26*).

Conformer **10a** can convert to **10d** via pathways involving intermediate rotamers **10b/b′** or **10c/c′**. Rotamers **10b/b′** are accessed by rotation of the thioester group in a clockwise movement about the C4−O5 bond relative to the C2−C3 bond, while **10c/c′** are accessed by rotation in the opposite direction. The pathway involving **10b/b′** is markedly lower in energy than that involving **10c/c′**, which can be attributed to intramolecular steric effects and hydrogen bonding. Rotamer **10c′** experiences a repulsive steric interaction manifested between the $-SCH_3$ group and the ethyl group (Figure 3), which accounts for a significant destabilization (14.7 kcal/mol) relative to **10a**. The predicted pathway for the conversion of **10a** to **10d** involves rotamers **10b/b′** since along with a decreased steric resistance, an accompanying stabilizing hydrogen bonding interaction is observed (**10b′**). The oxygen−hydroxy hydrogen bond distance of **10b′** is 2.045 Å, which is shorter than the hydrogen bond length of 2.74 Å reported for the X-ray crystal structure *p*-nitroperoxybenzoic acid (*29*). Since the energies of conformers **10b′** and **10d** lie within 4.4 kcal/mol of each other, possible collapse to the dithiolanone oxide surface via intermediate **10d** would reflect the outcome of a competition between the intramolecular S1−S5 interaction of **10d** and the OH−O5 hydrogen bonding interaction of **10b′**. The effect of the 1,5-S−X interaction in **10a** and **10d** is observed to a reduced extent compared to intermediates **10b/b′** and **10c/c′**. The most important factor that distinguishes the S−O **10a** from the S−S **10d** system in the gas phase is the stronger through-space interaction of the former, which is a consequence of the greater electronegativity of apical O compared to apical S.

Since the disposition of the 1,5-S−O interaction in **5** and **6** is clearly visible by X-ray crystallography (*3*), computations were conducted to probe this structural feature. The B3LYP calculated geometry from the S−O interaction of **10a** was transposed into the macrocycle of

Scheme 8

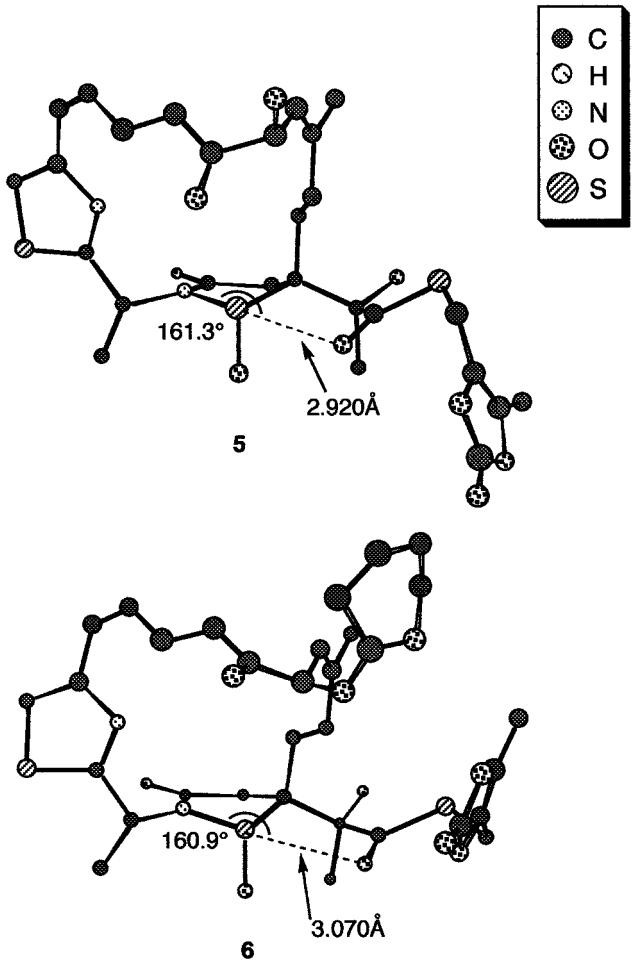

5 and **6** followed by a constrained optimization[3] at the PM3 level (Scheme 8). This procedure is used because B3LYP calculations on macrocycles **5** and **6** are prohibitively long and can be justified by comparison of the quality of the computational data to the quality of a fully optimized model system **9**. By exploring the 1,5-S−O interaction computationally, we find it plays a major role in determining the structural character of isothiazolidinone oxides **5** and **6**. The heterocycle structures exhibit five bonds at S1. The calculations indicate that the S1 and O5 atoms of **5** and **6** are in close contact (2.920 Å for **5** and 3.070 Å for **6**). As in the model systems above, the S1 atoms of **5** and **6** have expanded octets due to the coordination of the oxygen (O5) from the thioester. The N1−S1−O5 bond angle is found to be 161.3° for **5** and 160.9° for **6**.

Conclusion

The intramolecular through-space S−X interactions (X being oxygen or sulfur) between an adjacent thioester and the 3-isothiazolidinone 1-oxide heterocycle are described. This study incorporates theoretical calculations along with previous experimental X-ray data to provide evi-

[3] The calculated values are similar to those observed in the published X-ray crystal structures of **5** and **6** (*3*). The X-ray coordinates are not available from ref *3*; however, a request of the coordinates has been placed to these authors. The dihedral angle θ (S1−C2−C4−O5) was fixed at 11° for **5** and 5° for **6** (see **10a** in Scheme 7 for atom numbering). The dihedral angle θ is positive for a clockwise movement from S1 to O5 as you look down C2 to C4.

dence that the isothiazolidinone oxide surface depends on 1,5-S−X interactions, which may point to significance to biochemical reactions involving the generation of dithiolanone oxides. Gas phase calculations predict a dependence on dipole−dipole interactions and intramolecular hydrogen bonds. The relevance of the S−O and S−S interactions is predicted to be reduced with the inclusion of solvent effects partly because of a potential for specific hydrogen bonding interaction with the solute. The stability of the structure is sensitive to the identity of the apical ligand X. The energetic difference between the S−O and S−S interactions is ascribed to the preference for the apical position of oxygen compared to sulfur attained with the trigonal bipyramidal (TBP) geometry. An important aspect of this chemistry is the sensitivity of the S−X interaction to sterics, which may become an important issue in identifying isothiazolidinone oxide target prodrugs susceptible to conversion to dithiolanone oxide drugs.

Acknowledgment. We acknowledge a grant from the Petroleum Research Fund, administered by the American Chemical Society, and a research award from PSC-CUNY. Computer time was provided by the National Partnership for Advanced Computational Infrastructure and the San Diego Super Computer Center.

References

(1) Hara, M., Saitoh, Y., and Nakano, H. (1990) DNA Strand Scission by the Novel Antitumor Antibiotic Leinamycin. *Biochemistry* **29**, 5676−5681.

(2) Behroozi, S. J., Kim, W., Dannaldson, J., and Gates, K. S. (1996) 1,2-Dithiolano-3-one 1-Oxides. A Class of Thiol-Activated DNA-Cleaving Agents That Are Structurally Related to the Natural Product Leinamycin. *Biochemistry* **35**, 1768−1774.

(3) Kanda, Y., Ashizawa, T., Kakita, S., Takahashi, Y., Kono, M., Yoshida, M., Saitoh, Y., and Okabe, M. (1999) Synthesis and Antitumor Activity of Novel Thioester Derivatives of Leinamycin. *J. Med. Chem.* **42**, 1330−1332.

(4) Pattenden, G., and Thom, S. M. (1993) Polyene macrolactam construction using a Stille vinyl-vinyl coupling protocol: an approach to the antitumor antibiotic substance leinamycin. *Synlett*, 215−216.

(5) Yamada, H., Takahashi, T., Kanda, Y., Saitoh, Y., and Fukuyama, T. (1996) Stereoselective intramolecular Michael reaction of the 18-membere α,β-unsaturated macrolactam: MM2 transition structure models. *Heterocycles* **43**, 267−270.

(6) Kanda, Y., Ashizawa, T., Saitoh, Y., Saito, H., Gomi, K., and Okabe, M. (1998) Synthesis and antitumor activity of leinamycin derivatives: Modifications of C-8 hydroxy and C-9 keto groups. *Bioorg. Med. Chem. Lett.* **8**, 909−912.

(7) Mitra, K., Kim, W., Daniels, J. S., and Gates, K. S. (1997) Oxidative DNA Cleavage by the Antitumor Antibiotic Leinamycin and Simple 1,2-Dithiolan-3-one 1-Oxides: Evidence for Thiol-Dependent Conversion of Molecular Oxygen to DNA-Cleaving Radicals Mediated by Polysulfides. *J. Am. Chem. Soc.* **119**, 11691−11692.

(8) Asai, A., Hara, M., Kakita, S., Kanda, Y., Yoshida, M., Saito, H., and Saitoh, Y. (1996) Thiol-Mediated DNA Alkylation by the Novel Antitumor Antibiotic Leinamycin. *J. Am. Chem. Soc.* **118**, 6802−6803.

(9) Asai, A., Saito, H., and Saitoh, Y. (1997) Thiol-independent DNA cleavage by a leinamycin degradation product. *Bioorg. Med. Chem.* **5**, 723−729.

(10) Cambridge X-ray Crystallographic Data Base (1997) Cambridge, U.K.

(11) Burling, F. T., and Goldstein, B. M. (1992) Computational Studies of Nonbonded Sulfur−Oxygen and Selenium−Oxygen Interactions in the Thiazole and Selenazole Nucleosides. *J. Am. Chem. Soc.* **114**, 2313−2320.

(12) Burling, F. T., and Goldstein, B. M. (1993) A database study of nonbonded intramolecular sulfur-nucleophile contacts. *Acta Crystallogr.* **B49**, 738−744.

(13) Goldstein, B. M., Takusagawa, F., and Berman, H. M. (1983) Structural Studies of a New Antitumor Agent: Tiazofurin and Its Inactive Analogs. *J. Am. Chem. Soc.* **105**, 7416−7422.

(14) Nagao, Y. H. T., Goto, S., Sano, S., Kakehi, A., Iizuka, K., and Shiro, M. (1998) Intramolecular Nonbonded S−O Interaction Recognized in (Acylimino)thiadiazoline Derivatives as Angiotensin II Receptor Antagonists and Related Compounds. *J. Am. Chem. Soc.* **120**, 3104−3110.

(15) Wu, S., and Greer, A. (2000) Attractive Through-Space S−O Interaction in the DNA-Cleaving Antitumor Antibiotic Leinamycin. *J. Org. Chem.* **65**, 4883−4887.

(16) Frisch, M. J., Trucks, G. W., Schlegel, H. B., Gill, P. M. W., Johnson, B. G., Robb, M. A., Cheeseman, J. R., Keith, T., Petersson, G. A., Montgomery, J. A., Raghavachari, K., Al-Laham, M. A., Zakrzewski, V. G., Ortiz, J. V., Foresman, J. B., Cioslowski, J., Stefanov, B. B., Nanayakkara, A., Challacombe, M., Peng, C. Y., Ayala, P. Y., Chen, W., Wong, M. W., Andres, J. L., Replogle, E. S., Gomperts, R., Martin, R. L., Fox, D. J., Binkley, J. S., Defrees, D. J., Baker, J., Stewart, J. P., Head-Gordon, M., Gonzalez, C., and Pople, J. A. (1994) *Gaussian 94*, Gaussian, Inc., Pittsburgh.

(17) Miertus, S., Scrocco, E., and Tomasi, J. (1981) Electrostatic Interaction of a Solute with a Continuum. A Direct Utilization of ab initio Molecular Potentials for the Prevision of Solvent Effects. *Chem. Phys.* **55**, 117−129.

(18) Miertus, S., and Tomasi, J. (1982) Approximate Evaluations of the Electrostatic Free Energy and Internal Energy Changes in Solution Processes. *Chem. Phys.* **65**, 239−245.

(19) Van Meervelt, L. B., and Dehaen, W. (1997) X-ray Crystal Structure Analysis of 2-Methyl-4-*tert*-Butyl-1,2,3-Thiadiazol-5(2*H*)-ylidene Methyl Acetate. *Bull. Soc. Chim. Belg.* **106**, 641−642.

(20) Pauling, L. (1960) *The Nature of the Chemical Bond*, 3rd ed., Cornell University Press, Ithaca, NY.

(21) Krische, B., Walter, W., and Adiwidjaja, G. (1982) Kristall und Molekulstruktur eines bestandigen cyclischen Sulfenylcarboxylats ohne "bond-no bond"-Resonanz-Satbilisierung. *Chem. Ber.* **115**, 3842−3850.

(22) Iwasaki, F., and Furukawa, N. (1987) Structure of 1-tosylimino-1,5-dithiacyclooctane. *Acta Crystallogr.* **C43**, 80−83.

(23) Hayes, R. A., and Martin, J. C. (1985) *Organic Sulfur Chemistry. Theoretical and Experimental Advances*, Vol. 19, pp 408−483, Elsevier, Amsterdam.

(24) Kucsman, A., and Kapovits, I. (1985) *Organic Sulfur Chemistry. Theoretical and Experimental Advances*, Vol. 19., pp 191−245, Elsevier, Amsterdam.

(25) Trippett, S. (1976) Apicophilicity and Ring-Strain in Five-Coordinate Phosphoranes. *Phosphorus Sulfur* **73**, 89−98.

(26) Corbridge, D. E. C. (1990) *Phosphorus: An Outline of its Chemistry, Biochemistry, and Technology*, 4th ed., Chapter 14, pp 994−1007, Elsevier, Amsterdam.

(27) Wiberg, K. B., Rablen, P. R., Rush, D. J., and Keith, T. A. (1995) Amides 3. Experimental and Theoretical Studies of the Effect of Medium on the Rotational Barrier for *N*,*N*-Dimethylformamide and *N*,*N*-Dimethylacetamide. *J. Am. Chem. Soc.* **117**, 4261−4270.

(28) Wiberg, K. B., Keith, T. A., Frisch, M. J., and Murcko, M. (1995) Solvent Effects on 1,2-Dihaloethane Gauche/Trans Ratios. *J. Phys. Chem.* **99**, 9072−9079.

(29) Kim, H. S., Chu, S.-C., and Jeffery, G. A. (1970) The Crystal Structure of *p*-Nitroperoxybenzoic Acid. *Acta Crystallogr.* **B26**, 896−900.

TX000126+